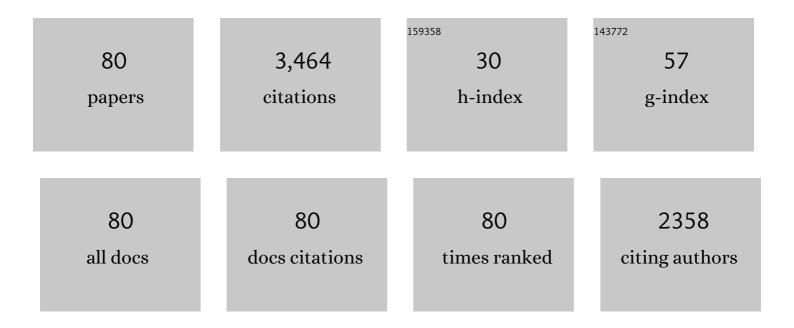
List of Publications by Year in descending order

Source: https://exaly.com/author-pdf/2320381/publications.pdf Version: 2024-02-01



#	Article	IF	CITATIONS
1	An Automatic Radiometric Cross-Calibration Method for Wide-Angle Medium-Resolution Multispectral Satellite Sensor Using Landsat Data. IEEE Transactions on Geoscience and Remote Sensing, 2022, 60, 1-11.	2.7	3
2	LiDAR-guided stereo matching with a spatial consistency constraint. ISPRS Journal of Photogrammetry and Remote Sensing, 2022, 183, 164-177.	4.9	13
3	Asymmetric Hash Code Learning for Remote Sensing Image Retrieval. IEEE Transactions on Geoscience and Remote Sensing, 2022, 60, 1-14.	2.7	22
4	KLGCN: Knowledge graph-aware Light Graph Convolutional Network for recommender systems. Expert Systems With Applications, 2022, 195, 116513.	4.4	11
5	LNIFT: Locally Normalized Image for Rotation Invariant Multimodal Feature Matching. IEEE Transactions on Geoscience and Remote Sensing, 2022, 60, 1-14.	2.7	27
6	Multi-Modal Remote Sensing Image Matching Considering Co-Occurrence Filter. IEEE Transactions on Image Processing, 2022, 31, 2584-2597.	6.0	50
7	DKDFN: Domain Knowledge-Guided deep collaborative fusion network for multimodal unitemporal remote sensing land cover classification. ISPRS Journal of Photogrammetry and Remote Sensing, 2022, 186, 170-189.	4.9	50
8	Combining deep learning and ontology reasoning for remote sensing image semantic segmentation. Knowledge-Based Systems, 2022, 243, 108469.	4.0	34
9	Water body classification from high-resolution optical remote sensing imagery: Achievements and perspectives. ISPRS Journal of Photogrammetry and Remote Sensing, 2022, 187, 306-327.	4.9	31
10	Few-Shot Scene Classification of Optical Remote Sensing Images Leveraging Calibrated Pretext Tasks. IEEE Transactions on Geoscience and Remote Sensing, 2022, 60, 1-13.	2.7	13
11	Error-Tolerant Deep Learning for Remote Sensing Image Scene Classification. IEEE Transactions on Cybernetics, 2021, 51, 1756-1768.	6.2	86
12	Simultaneous Cloud Detection and Removal From Bitemporal Remote Sensing Images Using Cascade Convolutional Neural Networks. IEEE Transactions on Geoscience and Remote Sensing, 2021, 59, 732-748.	2.7	52
13	Image retrieval from remote sensing big data: A survey. Information Fusion, 2021, 67, 94-115.	11.7	130
14	A Learnable Joint Spatial and Spectral Transformation for High Resolution Remote Sensing Image Retrieval. IEEE Journal of Selected Topics in Applied Earth Observations and Remote Sensing, 2021, 14, 8100-8112.	2.3	7
15	Learning Deep Cross-Modal Embedding Networks for Zero-Shot Remote Sensing Image Scene Classification. IEEE Transactions on Geoscience and Remote Sensing, 2021, 59, 10590-10603.	2.7	48
16	Unsupervised Building Instance Segmentation of Airborne LiDAR Point Clouds for Parallel Reconstruction Analysis. Remote Sensing, 2021, 13, 1136.	1.8	14
17	Learning deep semantic segmentation network under multiple weakly-supervised constraints for cross-domain remote sensing image semantic segmentation. ISPRS Journal of Photogrammetry and Remote Sensing, 2021, 175, 20-33.	4.9	119
18	SemiCDNet: A Semisupervised Convolutional Neural Network for Change Detection in High Resolution Remote-Sensing Images. IEEE Transactions on Geoscience and Remote Sensing, 2021, 59, 5891-5906.	2.7	148

#	Article	IF	CITATIONS
19	Robust deep alignment network with remote sensing knowledge graph for zero-shot and generalized zero-shot remote sensing image scene classification. ISPRS Journal of Photogrammetry and Remote Sensing, 2021, 179, 145-158.	4.9	78
20	Robust 3-D Plane Segmentation From Airborne Point Clouds Based on <i>Quasi-A-Contrario</i> Theory. IEEE Journal of Selected Topics in Applied Earth Observations and Remote Sensing, 2021, 14, 7133-7147.	2.3	9
21	Representation Learning of Remote Sensing Knowledge Graph for Zero-Shot Remote Sensing Image Scene Classification. , 2021, , .		6
22	Accurate cloud detection in high-resolution remote sensing imagery by weakly supervised deep learning. Remote Sensing of Environment, 2020, 250, 112045.	4.6	125
23	Multi-Label Remote Sensing Image Scene Classification by Combining a Convolutional Neural Network and a Graph Neural Network. Remote Sensing, 2020, 12, 4003.	1.8	48
24	Gated Convolutional Networks for Cloud Removal From Bi-Temporal Remote Sensing Images. Remote Sensing, 2020, 12, 3427.	1.8	17
25	Band-Independent Encoder–Decoder Network for Pan-Sharpening of Remote Sensing Images. IEEE Transactions on Geoscience and Remote Sensing, 2020, 58, 5208-5223.	2.7	12
26	Registration of Multimodal Remote Sensing Images Using Transfer Optimization. IEEE Geoscience and Remote Sensing Letters, 2020, 17, 2060-2064.	1.4	10
27	A CNN-GCN Framework for Multi-Label Aerial Image Scene Classification. , 2020, , .		9
28	Matching Confidence Constrained Bundle Adjustment for Multi-View High-Resolution Satellite Images. Remote Sensing, 2020, 12, 20.	1.8	13
29	Unsupervised Style Transfer via Dualgan for Cross-Domain Aerial Image Classification. , 2020, , .		1
30	End-to-End Change Detection for High Resolution Satellite Images Using Improved UNet++. Remote Sensing, 2019, 11, 1382.	1.8	435
31	A Lightweight and Discriminative Model for Remote Sensing Scene Classification With Multidilation Pooling Module. IEEE Journal of Selected Topics in Applied Earth Observations and Remote Sensing, 2019, 12, 2636-2653.	2.3	86
32	Building Instance Change Detection from Large-Scale Aerial Images using Convolutional Neural Networks and Simulated Samples. Remote Sensing, 2019, 11, 1343.	1.8	113
33	Pan-Sharpening Using an Efficient Bidirectional Pyramid Network. IEEE Transactions on Geoscience and Remote Sensing, 2019, 57, 5549-5563.	2.7	100
34	TopoLAP: Topology Recovery for Building Reconstruction by Deducing the Relationships between Linear and Planar Primitives. Remote Sensing, 2019, 11, 1372.	1.8	25
35	An a-contrario method of mismatch detection for two-view pushbroom satellite images. ISPRS Journal of Photogrammetry and Remote Sensing, 2019, 153, 123-136.	4.9	7
36	A Mixture Likelihood Model of the Anisotropic Gaussian and Uniform Distributions for Accurate Oblique Image Point Matching. IEEE Geoscience and Remote Sensing Letters, 2019, 16, 1437-1441.	1.4	1

#	Article	IF	CITATIONS
37	A Coarse-to-Fine Framework for Cloud Removal in Remote Sensing Image Sequence. IEEE Transactions on Geoscience and Remote Sensing, 2019, 57, 5963-5974.	2.7	31
38	Automatic and Unsupervised Water Body Extraction Based on Spectral-Spatial Features Using GF-1 Satellite Imagery. IEEE Geoscience and Remote Sensing Letters, 2019, 16, 927-931.	1.4	23
39	Object-Based Change Detection for VHR Images Based on Multiscale Uncertainty Analysis. IEEE Geoscience and Remote Sensing Letters, 2018, 15, 13-17.	1.4	73
40	Large-Scale Remote Sensing Image Retrieval by Deep Hashing Neural Networks. IEEE Transactions on Geoscience and Remote Sensing, 2018, 56, 950-965.	2.7	209
41	Robust infrared small target detection using local steering kernel reconstruction. Pattern Recognition, 2018, 77, 113-125.	5.1	87
42	Deep networks under scene-level supervision for multi-class geospatial object detection from remote sensing images. ISPRS Journal of Photogrammetry and Remote Sensing, 2018, 146, 182-196.	4.9	111
43	Adaptive Image Mismatch Removal With Vector Field Interpolation Based on Improved Regularization and Gaussian Kernel Function. IEEE Access, 2018, 6, 55599-55613.	2.6	4
44	Salient Object Detection via Recursive Sparse Representation. Remote Sensing, 2018, 10, 652.	1.8	14
45	Fine Registration for VHR Images Based on Superpixel Registration-Noise Estimation. IEEE Geoscience and Remote Sensing Letters, 2018, , 1-5.	1.4	2
46	Two-Pass Robust Component Analysis for Cloud Removal in Satellite Image Sequence. IEEE Geoscience and Remote Sensing Letters, 2018, 15, 1090-1094.	1.4	19
47	Learning Source-Invariant Deep Hashing Convolutional Neural Networks for Cross-Source Remote Sensing Image Retrieval. IEEE Transactions on Geoscience and Remote Sensing, 2018, 56, 6521-6536.	2.7	126
48	3D building roof reconstruction from airborne LiDAR point clouds: a framework based on a spatial database. International Journal of Geographical Information Science, 2017, 31, 1359-1380.	2.2	34
49	A Mixed Radiometric Normalization Method for Mosaicking of High-Resolution Satellite Imagery. IEEE Transactions on Geoscience and Remote Sensing, 2017, 55, 2972-2984.	2.7	23
50	Object-based change detection from satellite imagery by segmentation optimization and multi-features fusion. International Journal of Remote Sensing, 2017, 38, 3886-3905.	1.3	28
51	An auto-adapting global-to-local color balancing method for optical imagery mosaic. ISPRS Journal of Photogrammetry and Remote Sensing, 2017, 132, 1-19.	4.9	24
52	The P2L method of mismatch detection for push broom high-resolution satellite images. ISPRS Journal of Photogrammetry and Remote Sensing, 2017, 130, 317-328.	4.9	9
53	A Two-Step Semiglobal Filtering Approach to Extract DTM From Middle Resolution DSM. IEEE Geoscience and Remote Sensing Letters, 2017, 14, 1599-1603.	1.4	7
54	A Simple and Efficient Method for Radial Distortion Estimation by Relative Orientation. IEEE Transactions on Geoscience and Remote Sensing, 2017, 55, 6840-6848.	2.7	1

#	Article	IF	CITATIONS
55	Direct Digital Surface Model Generation by Semi-Global Vertical Line Locus Matching. Remote Sensing, 2017, 9, 214.	1.8	11
56	Content-Based High-Resolution Remote Sensing Image Retrieval via Unsupervised Feature Learning and Collaborative Affinity Metric Fusion. Remote Sensing, 2016, 8, 709.	1.8	62
57	Cloud Extraction from Chinese High Resolution Satellite Imagery by Probabilistic Latent Semantic Analysis and Object-Based Machine Learning. Remote Sensing, 2016, 8, 963.	1.8	36
58	Automatic Keyline Recognition and 3D Reconstruction For Quasiâ€Planar Façades in Closeâ€range Images. Photogrammetric Record, 2016, 31, 29-50.	0.4	6
59	A novel spatio-temporal saliency approach for robust dim moving target detection from airborne infrared image sequences. Information Sciences, 2016, 369, 548-563.	4.0	57
60	Colour balancing of satellite imagery based on a colour reference library. International Journal of Remote Sensing, 2016, 37, 5763-5785.	1.3	10
61	DEM-Aided Bundle Adjustment With Multisource Satellite Imagery: ZY-3 and GF-1 in Large Areas. IEEE Geoscience and Remote Sensing Letters, 2016, 13, 880-884.	1.4	16
62	A combined image matching method for Chinese optical satellite imagery. International Journal of Digital Earth, 2016, 9, 851-872.	1.6	10
63	DEM-Assisted RFM Block Adjustment of Pushbroom Nadir Viewing HRS Imagery. IEEE Transactions on Geoscience and Remote Sensing, 2016, 54, 1025-1034.	2.7	27
64	Extracting buildings from and regularizing boundaries in airborne lidar data using connected operators. International Journal of Remote Sensing, 2016, 37, 889-912.	1.3	33
65	Optimized 3D Street Scene Reconstruction from Driving Recorder Images. Remote Sensing, 2015, 7, 9091-9121.	1.8	11
66	Multistrip Bundle Block Adjustment of ZY-3 Satellite Imagery by Rigorous Sensor Model Without Ground Control Point. IEEE Geoscience and Remote Sensing Letters, 2015, 12, 865-869.	1.4	44
67	Self-Calibration Adjustment of CBERS-02B Long-Strip Imagery. IEEE Transactions on Geoscience and Remote Sensing, 2015, 53, 3847-3854.	2.7	14
68	LiDAR Strip Adjustment Using Multifeatures Matched With Aerial Images. IEEE Transactions on Geoscience and Remote Sensing, 2015, 53, 976-987.	2.7	36
69	Fully automatic generation of geoinformation products with chinese zyâ€3 satellite imagery. Photogrammetric Record, 2014, 29, 383-401.	0.4	13
70	On-Orbit Geometric Calibration of ZY-3 Three-Line Array Imagery With Multistrip Data Sets. IEEE Transactions on Geoscience and Remote Sensing, 2014, 52, 224-234.	2.7	75
71	Technologies and system for automatic generation of advanced geo-spatial products with Chinese satellite imagery. Proceedings of SPIE, 2014, , .	0.8	Ο
72	Direct georeferencing of airborne LiDAR data in national coordinates. ISPRS Journal of Photogrammetry and Remote Sensing, 2013, 84, 43-51.	4.9	15

#	Article	IF	CITATIONS
73	Combined Bundle Block Adjustment with Spaceborne Linear Array and Airborne Frame Array Imagery. Photogrammetric Record, 2013, 28, 162-177.	0.4	3
74	A New Approach on Optimization of the Rational Function Model of High-Resolution Satellite Imagery. IEEE Transactions on Geoscience and Remote Sensing, 2012, 50, 2758-2764.	2.7	44
75	Photogrammetric processing of lowâ€altitude images acquired by unpiloted aerial vehicles. Photogrammetric Record, 2011, 26, 190-211.	0.4	69
76	Photogrammetric Modeling of Linear Features with Generalized Point Photogrammetry. Photogrammetric Engineering and Remote Sensing, 2008, 74, 1119-1127.	0.3	24
77	Photogrammetric Modeling of Linear Features with Generalized Point Photogrammetry. Photogrammetric Engineering and Remote Sensing, 2007, 73, 1119-1127.	0.3	12
78	3D Building Modelling with Digital Map, Lidar Data and Video Image Sequences. Photogrammetric Record, 2005, 20, 285-302.	0.4	43
79	Deformation visual inspection of industrial parts with image sequence. Machine Vision and Applications, 2004, 15, 115.	1.7	10
80	IMAGE-GUIDED NON-LOCAL DENSE MATCHING WITH THREE-STEPS OPTIMIZATION. ISPRS Annals of the Photogrammetry, Remote Sensing and Spatial Information Sciences, 0, III-3, 67-74.	0.0	5